JCB Article

Back signaling by the Nrg-1 intracellular domain

Jianxin Bao,[1,3] Deon Wolpowitz,[3] Lorna W. Role,[1,3] and David A. Talmage[2,4]

[1]Department of Anatomy and Cell Biology, [2]Department of Pediatrics, [3]Center for Neurobiology and Behavior, and [4]Institute of Human Nutrition, Columbia University, New York, NY 10032

Transmembrane isoforms of neuregulin-1 (Nrg-1), ligands for erbB receptors, include an extracellular domain with an EGF-like sequence and a highly conserved intracellular domain (ICD) of unknown function. In this paper, we demonstrate that transmembrane isoforms of Nrg-1 are bidirectional signaling molecules in neurons. The stimuli for Nrg-1 back signaling include binding of erbB receptor dimers to the extracellular domain of Nrg-1 and neuronal depolarization. These stimuli elicit proteolytic release and translocation of the ICD of Nrg-1 to the nucleus. Once in the nucleus, the Nrg-1 ICD represses expression of several regulators of apoptosis, resulting in decreased neuronal cell death in vitro. Thus, regulated proteolytic processing of Nrg-1 results in retrograde signaling that appears to mediate contact and activity-dependent survival of Nrg-1–expressing neurons.

Introduction

The neuregulin-1 (Nrg-1)* gene encodes multiple isoforms of ligands for erbB receptor tyrosine kinases (Pinkas-Kramarski et al., 1998; Buonanno and Fischbach, 2001; Murphy et al., 2002). Many of these Nrg-1 isoforms are membrane-anchored growth factors consisting of variable NH_2-terminal extracellular domains (ECDs) and conserved transmembrane and COOH-terminal cytoplasmic domains (Buonanno and Fischbach, 2001). Interactions between the ECD of Nrg-1 and erbB receptor tyrosine kinases can occur after release of the Nrg-1 ECD, either directly after synthesis of isoforms lacking transmembrane domains or after proteolysis of the transmembrane precursor form. Nrg-1–erbB interactions also can occur within the context of cell–cell contact (Aguilar and Slamon, 2001; Leimeroth et al., 2002). Genetic analyses have demonstrated that Nrg-1 function is essential during embryonic development, and have identified Nrg-1 isoform–specific functions. Genetic disruptions in mice that prevent expression of all Nrg-1 isoforms result in defects in cardiac development and embryonic lethality at E10 (Lee et al., 1995; Meyer and Birchmeier, 1995; Carraway, 1996; Kramer et al., 1996; Liu et al., 1998a). Disruption of type III isoforms that contain an NH_2-terminal, cysteine-rich domain (CRD; i.e., CRD-Nrg-1), whose expression is restricted to the nervous system, results in perinatal lethality (Yang et al., 1998b; Wolpowitz et al., 2000). These neuronal CRD-Nrg-1s are required for the formation and stable maintenance of functional motor and sensory synapses.

A striking feature of the phenotype of CRD-Nrg-$1^{-/-}$ mice is the progressive loss of the motor and sensory neurons that would normally express the CRD-Nrg-1 growth factor (Wolpowitz et al., 2000). In CRD-Nrg-$1^{-/-}$ mice, neuron loss occurs only after the neurons enter target fields. In the target fields, these neurons initiate the formation of contacts, but fail to sustain synaptic interactions. Thus, it appears that CRD-Nrg-1 interactions with erbB receptors elicit a signal required for the survival of the CRD-Nrg-1–expressing cell. The nature and origin of this signal is unknown. One possibility is that CRD-Nrg-1 activation of erbB signaling stimulates the release of a soluble factor that interacts with receptors on the surface of neurons. An alternative explanation is that a CRD-Nrg-1–erbB complex signals bidirectionally via erbB kinase activity in the "forward" direction and the CRD-Nrg-1 intracellular domain (ICD; i.e., Nrg-1-ICD) in the "reverse" direction. Several lines of evidence support a signaling function for the Nrg-1-ICD. First, ectopic expression of Nrg-1 leads to Nrg-1-ICD–dependent apoptosis (Grimm and Leder, 1997; Grimm et al., 1998; Weinstein and Leder, 2000). Second, the Nrg-1-ICD forms specific complexes with cytoplasmic proteins, including LIM kinase (Wang et al., 1998) and a zinc finger protein of undetermined function (the cytoplasmic domain of Nrg-interacting protein [CNIP]; unpublished data). Third, the Nrg-1-ICD is required for Nrg-1 function in vivo (Liu et al., 1998a).

In this paper, we set out to address two questions. First, does interaction of cell surface CRD-Nrg-1 with erbB4

Address correspondence to David A. Talmage, Institute of Human Nutrition, 701 West 168th St., 5-503 New York, NY 10032. Tel.: (212) 305-2107. Fax: (212) 305-3079. E-mail: dat1@columbia.edu

*Abbreviations used in this paper: CRD, cysteine-rich domain; ECD, extracellular domain; ICD, intracellular domain; LIMK1, LIM kinase 1; Nrg-1, neuregulin-1.

Key words: erbB receptors; apoptosis; γ-secretase; synaptic maintenance; neurodegeneration

The Journal of Cell Biology, Volume 161, Number 6, June 23, 2003 1133–1141
http://www.jcb.org/cgi/doi/10.1083/jcb.200212085

The Journal of Cell Biology

ligand binding domain directly stimulate a survival signal in neurons? Second, do these interactions stimulate proteolytic release of a functional Nrg-1-ICD? We demonstrate that treating CRD-Nrg-1–expressing neurons with soluble forms of erbB ECDs promotes neuron survival in vitro and alters the expression of several apoptotic genes. Depolarization of the neurons appears to regulate gene expression in a similar manner, and either depolarization or treatment with soluble erbBs elicits translocation of the Nrg-1-ICD to the nucleus. Using transfected cells, we also demonstrate that the Nrg-1-ICD contains an amino acid motif required for nuclear targeting, that the Nrg-1-ICD has the ability to function as a transcriptional transactivator, and that compounds that inhibit γ-secretase activity alter the processing of the Nrg-1-ICD.

Results

Previously, we documented loss of CRD-Nrg-1–expressing motor and sensory neurons and cranial nerve nuclei in CRD-Nrg-1$^{-/-}$ mice (Wolpowitz et al., 2000). Loss of CRD-Nrg-1–expressing neurons in spiral ganglia (Fig. 1 A) and hippocampus (not depicted) also was evident in E16 CRD-Nrg-1$^{-/-}$ embryos. The fraction of the spiral ganglion volume and the CA3 region of the hippocampus occupied by neurons in wild-type or CRD-Nrg-1$^{-/-}$ embryos were evaluated from 12-μM serial sections stained for GAP43 expression. The fraction of neurons in mutant hippocampus (CA3 region) and mutant spiral ganglia (SG) were decreased by 50 and 90%, respectively (Fig. 1 A and not depicted). In contrast, evaluation of the erbB4-expressing cells within the target cochlea revealed that neither the number nor the distribution of erbB4-expressing cells (Co) was altered in mutant embryos (compared with wild-type; Fig. 1 A, top).

The observations that disrupting the CRD-Nrg-1 gene resulted in the loss of neurons that would have expressed CRD-Nrg-1 protein, led us to ask whether interactions between erbB receptors and CRD-Nrg-1 promotes neuronal survival. To test this idea, neurons were isolated from E16 mouse embryos, dispersed, and maintained in vitro. Apoptosis was evaluated by the presence of nuclear shrinkage and chromatin condensation after staining with bisbenzimide (Fig. 1 B, arrows). The fraction of neurons that were undergoing apoptosis 48 h after plating was 0.19–0.22 (Fig. 1, B and C, untreated and Nrg-ECD–treated controls). When neurons were incubated overnight in media containing soluble forms of the ECDs of erbB2 and erbB4 (which, together, constitute a high affinity receptor for Nrg-1; Fitzpatrick et al., 1998), the number of apoptotic neurons was reduced significantly (Fig. 1 C; *, $P < 0.01$). The protection against apoptosis was specific for erbB2:erbB4. Neither soluble erbB2 alone (which does not bind Nrg-1) nor the soluble erbB2:erbB4 preincubated with CRD-Nrg-1-ECD before treatment affected neuronal survival (fraction of apoptotic neurons: untreated controls, 0.21; CRD-Nrg-1-ECD, 0.20; erbB2:B4, 0.13; erbB2:B4 + CRD-Nrg-1-ECD, 0.17). Treatment with soluble erbBs also protected hippocampal neurons from staurosporine-induced apoptosis by ~50% (fraction apoptotic: untreated controls 0.2; staurosporine alone 0.62; staurosporine + erbB2:B4 0.38). In addition to

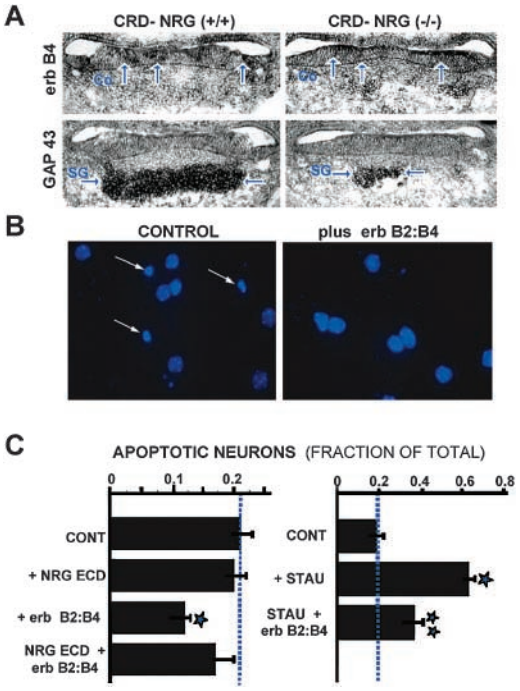

Figure 1. **Interaction between CRD-Nrg-1 and erbB receptors enhances survival of CRD-Nrg-1–expressing neurons.** (A) Spiral ganglion neurons are lost after genetic disruption of CRD-Nrg-1. Spiral ganglia from wild-type (left) or CRD-Nrg-1$^{-/-}$ mutant (right) E16.5 mouse embryos were hybridized to cRNA probes for either erbB4 (top) or GAP43 (to identify neurons). Based on 3-D reconstructions of serial sections, there was a 90% decrease in spiral ganglion neurons (GAP43 mRNA positive; SG) in mutant embryos. The erbB4-expressing cochlear epithelium (Co) was not measurably affected in the mutants. (B and C) Dispersed neurons were maintained in culture for 2 d and treated with soluble erbB2 + erbB4 (erbB2:B4), the CRD-Nrg-1 ECD (Nrg-ECD), a mixture of soluble erbB2:4 and Nrg-ECD, or staurosporine with or without soluble erbB2:B4. Apoptotic cells were visualized by staining nuclei with bisbenzimide (B, arrows). The percentage of total nuclei (±SEM) that appeared apoptotic was quantified in 10 fields from each treatment group in three independent experiments. Where indicated, values differed significantly ($P < 0.01$) from the untreated control group (*) or from the staurosporine-treated group (**).

the changes in the number of healthy versus dying neurons detected under these conditions, there were parallel changes in the percentage of cells with detectable immunoreactive Nrg-1-ICD, and the intensity of staining in general, and over nuclei in particular.

The apparent differences in localization and levels of Nrg-1 in erbB2:erbB4-treated cells were examined in greater detail (Fig. 2). Neuronal cultures were stained with antibodies recognizing the shared ECD of Nrg-1 or the COOH-terminal region of the longest ICD of Nrg-1 (Nrg-1-ICD; a-form). Both antibodies against Nrg-1-ECD and Nrg-1-ICD stained untreated cells in an overlapping distribution in all nonnuclear compartments. Immunoreactive Nrg-1 was more diffusely distributed in neuronal soma and along the processes of control neurons viewed at either the nuclear (Fig. 2 A, top left) or the neurite level (Fig. 2 A, bottom). Nonneuronal cells did not stain with Nrg-1 antibodies, and all immunostaining was completely blocked by preincubation of the antibodies with peptide antigen (Fig. 2 D). After treatment

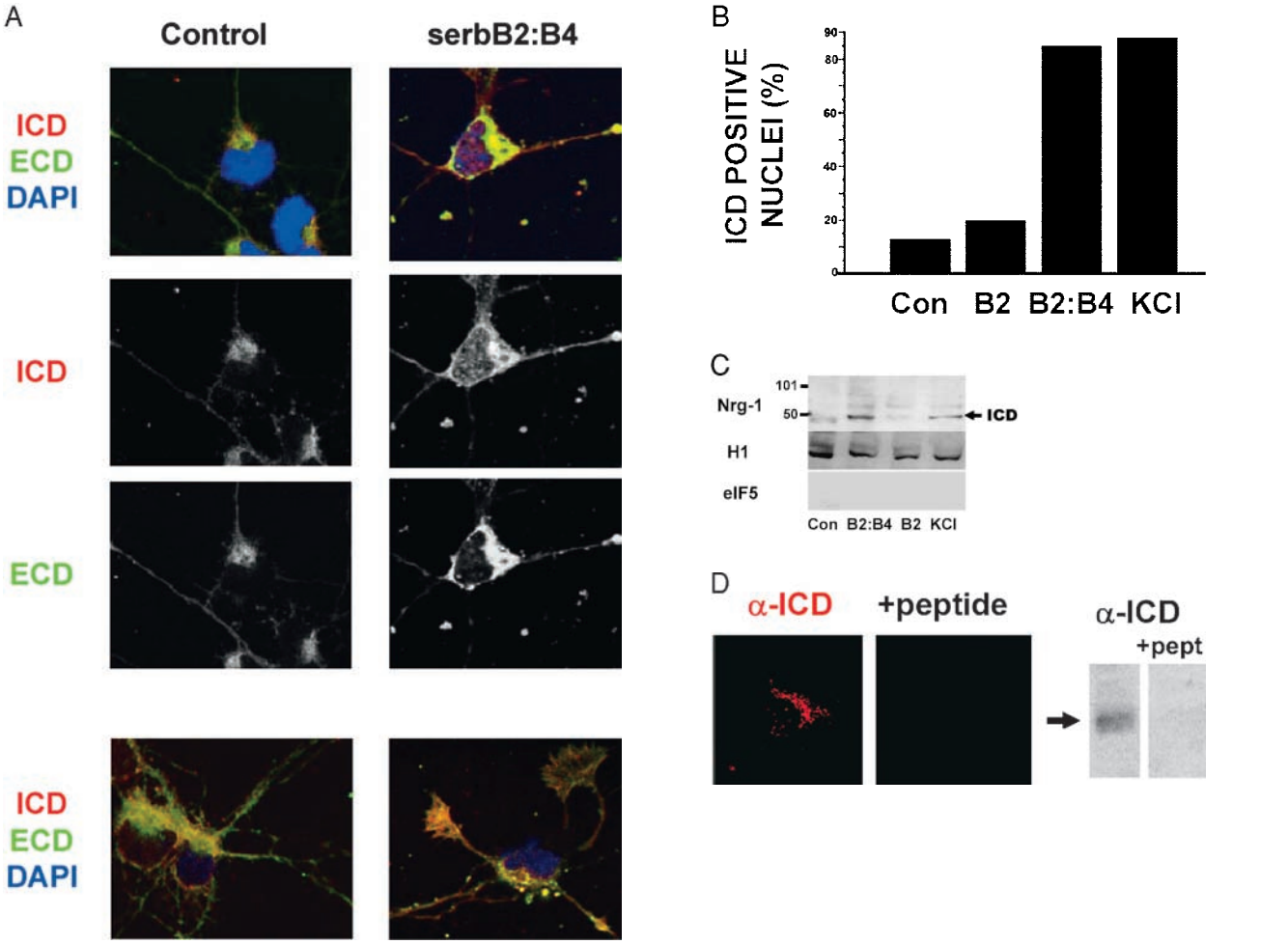

Figure 2. **Interaction with erbB receptors, or depolarization, target Nrg-1-ICD to the nucleus in primary neurons.** (A) Dispersed E16 spiral ganglion neurons were maintained in vitro for 3 d and stained with antibodies recognizing the ICD of the "a" form of Nrg-1 (red), or the ECD of all Nrg-1β isoforms (green). Nuclei were stained with DAPI (blue). 15 min before fixation and staining, neuronal cultures were either untreated (control) or treated with soluble erbB2:B4 (serbB2:B4). Fluorescent images in 1-μm sections were collected with a two-photon microscope. Under control conditions, intracellular and ECDs colocalize in soma and in processes. After treatment, colocalization is lost in neurites, both domains appear in clusters, and clusters of ICD staining are clearly present in the nucleus. The top six images are from 1-μm optical sections collected from the middle of the nuclei, whereas the bottom two images were collected at a level below the nuclei to emphasize the distribution of Nrg-1 in the processes. (B) The percentage of neuronal nuclei showing staining with the antibody recognizing the Nrg-1-ICD was quantified after a 15-min treatment with nothing (control), soluble erbB2 (which does not bind to Nrg-1), soluble erbB2 + erbB4 (erbB2:B4), or 50 mM KCl. Only cells showing clearly outlined nuclei were included in the analyses and at least 50 cells were scored per field. The data are plotted as the mean of the counts from two experiments. (C) Spiral ganglion neurons from six E13.5 embryos were maintained in culture overnight before treatment for 15 min with nothing (control), soluble erbB2 (B2), soluble erbB2 + erbB4 (B2:B4), or 50 mM KCl. Nuclear extracts (18 μg protein/lane) were resolved by SDS-PAGE, and Nrg-1-ICD was detected by probing immunoblots with the ICD antibody (sc-348). After stripping, the filters were reprobed sequentially with antibodies recognizing histone H1 (H1, nuclear marker) or the translation initiation factor eIF5 (eIF5, cytoplasmic marker). The anti–Nrg-1-ICD antibody recognized a protein of ~50 kD. Nuclei from cells treated with soluble erbB2:B4 or 50 mM KCl had significantly elevated levels of this 50-kD band. (D) Spiral ganglia neurons were treated for 15 min with soluble erbB2 + erbB4 and were either fixed and stained with antibody recognizing the Nrg-1-ICD (left) or lysed and analyzed by immunoblotting (right). Where indicated (+peptide, +pept), the primary antibody was preincubated with immunizing peptide before staining cells or probing filters. Preincubation eliminated staining of cells and staining of the 50-kD protein on immunoblots (+pept).

with soluble erbB2:B4, the Nrg-1 staining pattern changed in several ways. First, there was a decrease in diffuse staining along processes with both the extracellular and ICD antibodies. Second, diffuse staining was replaced by pronounced "patches" of immunoreactive Nrg-1 at various points along the processes. Third, there was an increase in somal staining, in particular of a Golgi-like area adjacent to nuclei. The patches and the Golgi-like staining were seen with both antibodies; and fourth, multiple discrete puncta were seen in nuclei (note that in Fig. 2 A, all images are from 1-μM sections captured through the middle of the nucleus, except for the neurite pictures in the bottom). These puncta stained with ICD antibody, but not with ECD antibody. Thus, within 20 min after treatment with soluble erbB2:erbB4, the intracellular and the ECDs separated and the ICD entered the nucleus.

The presence of strong patches of Nrg-1-ICD, but not Nrg-1-ECD, immunoreactivity in neuronal nuclei indicates that exposing neurons to soluble erbB2:erbB4 resulted in

physical separation of Nrg-1 ECD from Nrg-1 ICD. We postulated that such separation and subsequent nuclear targeting of the Nrg-1-ICD might participate in Nrg-1:erbB-induced signaling, which is implicated in the survival of neurons in vivo (Wolpowitz et al., 2000) and in vitro (Fig. 1). To verify, and to quantify the magnitude of this response, we measured the percentage of total neurons that had nuclear, immunoreactive Nrg-1-ICD under a variety of conditions. In untreated (control) cultures, 15–20% of neuronal nuclei were positive for Nrg-1-ICD staining. After 15 min of treatment with soluble erbB2:erbB4 or after 15 min of depolarization (see Materials and methods), >85% of nuclei stained positive for Nrg-1-ICD (Fig. 2 B). Treatment with soluble erbB2 alone did not affect nuclear staining.

To explore further the possibility that cell surface erbB–CRD-Nrg-1 interactions result in proteolytic release and nuclear translocation of the Nrg-1-ICD, we prepared nuclear fractions from dispersed neurons 15 min after treatment with erbB2, erbB2 + erbB4, or 50 mM KCl. Extract proteins were resolved electrophoretically and immunoblots were probed with the Nrg-1-ICD specific antibody (Fig. 2 C). A faint signal at ~50 kD was seen in nuclear extracts from untreated (control) or soluble erbB2-treated cells. Stimulation with either the soluble erbB2:erbB4 combination or with KCl elevated the amount of the ~50-kD band detected in nuclear extracts. Preincubating the antibody with immunizing peptide (Nrg-1 + pept) led to a loss of signal (Fig. 2 D). The size of this band is consistent with a peptide corresponding to the intracellular portion of Nrg-1a (see Fig. 4; for review see Wang et al., 2001).

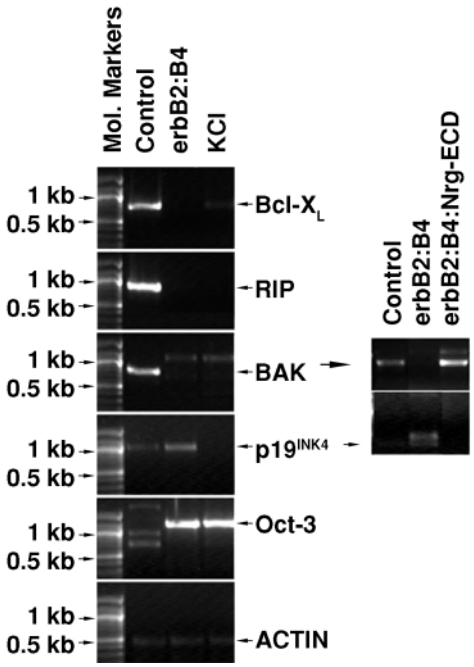

Figure 3. **Treatments that target Nrg-1-ICD to the nucleus alter gene expression.** E13.5 spiral ganglion neurons maintained in culture overnight were untreated (control) or stimulated with soluble erbB2:B4 or 50 mM KCl for 2 h. Total RNA was isolated and the relative levels of Bcl-X_L, RIP, BAK, p19^{INK4}, Oct-3, and actin mRNAs were determined by RT-PCR. Amplified products were resolved on agarose gels and visualized with ethidium bromide. Arrows indicate amplified products whose identities were verified by DNA sequencing (the additional bands in the treated BAK lanes and the untreated Oct-3 lanes were nonspecific amplification products). This experiment was repeated with soluble erbB2:B4 that had been preincubated with the ECD of CRD-Nrg-1 (right).

These results are consistent with regulated cleavage and release of the Nrg-1-ICD from the membrane and its subsequent translocation to the nucleus. Regulated intramembranous proteolysis of Notch (Struhl and Adachi, 2000; Struhl and Greenwald, 2001), SRE-BP1 and 2 (Brown and Goldstein, 1997; Brown et al., 2000), and possibly βAPP (Cao and Sudhof, 2001; Kimberly et al., 2001) and erbB4 (Ni et al., 2001; Lee et al., 2002) result in ICD-dependent regulation of gene expression. To determine whether regulated nuclear targeting of the Nrg-1-ICD was associated with changes in gene expression, we isolated total RNA from neuronal cultures that were either untreated or treated for 2 h with soluble erbB2 + erbB4. Using these RNAs, we synthesized ^{32}P-labeled cDNAs and probed a mouse cDNA array. Clear differences in expression of Oct-3, p19^{INK4}, IL-11, Bcl-X, BAK, and RIP were seen and confirmed by RT-PCR (Fig. 3). Expression of Bcl-X, BAK, and RIP were repressed after treatment with the soluble erbBs and after depolarization with KCl. Expression of Oct-3, p19^{INK4}, and IL-11 increased after treatment of neurons with erbB2 + erbB4, but only Oct-3 expression increased in response to KCl. Thus, although both depolarization and erbB2:erbB4 treatment induced nuclear translocation of Nrg-1-ICD, the effects of these treatments on target gene expression differed.

To confirm that the effects on gene expression seen after treatment of neuronal cultures with soluble erbB2 + erbB4 required the interaction of these proteins with the ECD of endogenously expressed Nrg-1, neuronal cultures were either untreated, treated with soluble erbB2 + erbB4, or treated with erbB2 + erbB4 that had been preincubated with the CRD-Nrg-1 ECD. Expression of BAK and p19^{INK4} were measured by RT-PCR analysis of total RNA. Preincubating erbB2 + erbB4 with CRD-Nrg-1 ECD blocked the effects on BAK and p19^{INK4} expression (Fig. 3).

To gain more insight into the dynamics of regulated nuclear targeting of the Nrg-1-ICD, we expressed a series of chimeric CRD-Nrg-1s in HEK 293T cells (Fig. 4). Subcellular targeting of Nrg-1 was followed in living cells transfected with a CRD-Nrg-1βa-GFP fusion protein by continuous monitoring of the distribution of GFP by collecting images through the z-axis of cells (Fig. 4 A). In control cells, the strongest CRD-Nrg-1-GFP signal was detected around the cell periphery and in a single intracellular region, consistent with previous reports of Nrg-1 localization in the plasma membrane, Golgi structure, and endoplasmic reticulum (Burgess et al., 1995). This pattern remained essentially unchanged for up to 2 h of continuous observation. In contrast, within 2–4 min after treatment with soluble erbB2 + erbB4, the distribution of green fluorescence changed and distinct fluorescent aggregates were seen both in peripheral regions of the cells and near Golgi-like structures. By 16 min after erbB2:erbB4 treatment, these GFP aggregates moved along discrete paths and entered the nucleus (Fig. 4, arrows).

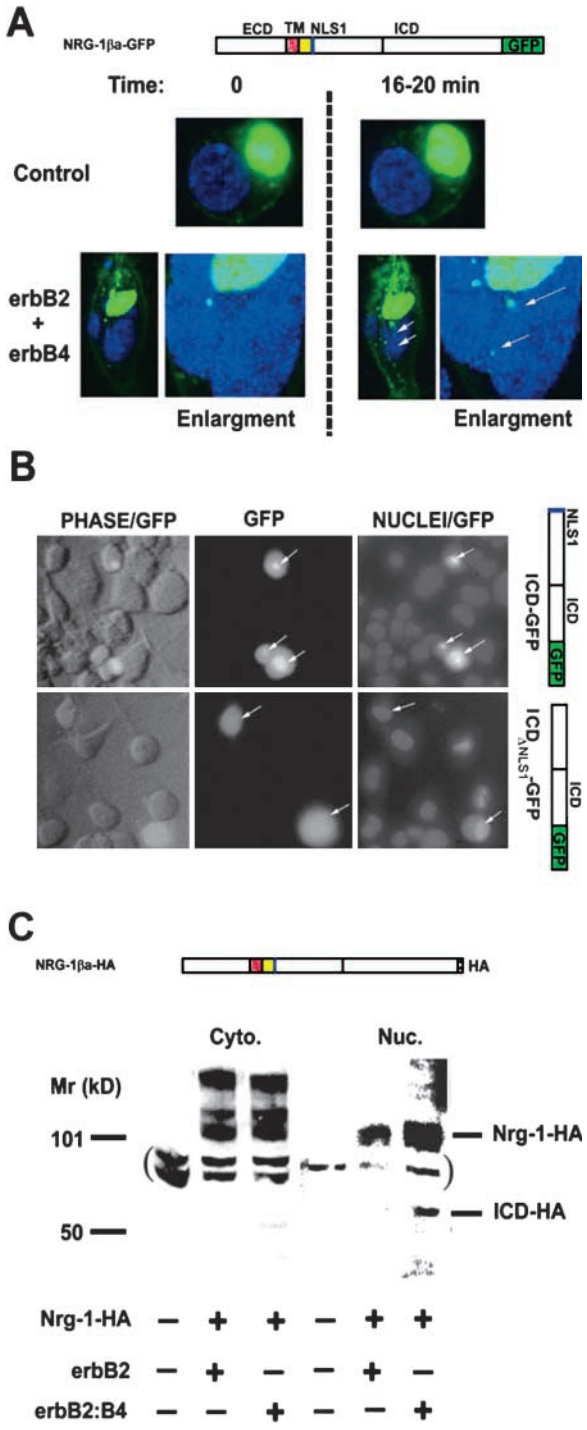

Figure 4. **Nuclear translocation of Nrg-1-ICD–GFP fusions can be visualized in living cells.** (A) The schematic illustration at the top shows the NRG-1βa-GFP chimeric used in this work. ECD, extracellular domain; TM, transmembrane domain; NLS1, the putative nuclear localization sequence (B); ICD, intracellular domain; GFP, green fluorescent protein. Intracellular movement of NRG-1βa-GFP was followed in live cells (HEK 293 cells) by two-photon microscopy. Images (1 μm from the middle of the nucleus) were collected at various intervals (min) after treatment with soluble erbB2 + erbB4. The arrows in the enlargement point out puncta of Nrg-1-GFP that have entered the nucleus. (B) HEK293 cells were transfected with plasmids encoding either an intact Nrg-1-ICD fused to GFP (top) or an Nrg-1-ICD lacking the putative NLS fused to GFP (bottom). The subcellular localization of the fusion proteins was followed by conventional fluorescence microscopy. At left are phase images. In the middle, the green fluorescence signal is shown (arrows point to positive cells), and at the right, both green fluorescence and DAPI staining are shown. (C) Cytoplasmic (Cyto) and nuclear (Nuc) fractions were prepared from mock-transfected or NRG-1βa-HA (HA, influenza virus hemagglutinin-derived epitope added to COOH terminus of Nrg-1)–transfected HEK293T cells. Proteins were analyzed by immunoblotting using antibodies recognizing the HA epitope. NRG-1βa-HA–transfected cells were treated for 15 min with erbB2 (32 μg/ml) or erbB2:4 (32 μg/ml). In addition to a doublet of nonspecific bands, proteins of >100 kD (full-length and aggregated NRG-1βa) and 50 kD (ICD-HA) were detected. The 50-kD band enriched in the nuclear fraction was only seen in cells treated with soluble erbB2:B4.

The induced targeting of Nrg-1-ICD to the nucleus indicated that the Nrg-1-ICD might contain an identifiable NLS. Inspection of the primary sequence of Nrg-1-ICDs identified two potential NLSs (http://psort.nibb.ac.jp). The first, NLS-1, includes the first eight amino acids after the transmembrane domain (KTKKQRKK) and is found in all Nrg-1-ICDs. We expressed Nrg-1-ICD-GFP fusion proteins that contained or lacked these eight amino acids in 293T cells (Fig. 4 B; these fusion proteins included just the ICD of Nrg-1 fused to GFP and lacked the transmembrane domain). Strong nuclear and diffuse cytoplasmic staining was seen when Nrg-1βc-ICD-GFP was expressed. Nrg-1βc-$ICD_{\Delta NLS1}$-GFP, lacking the eight–amino acid NLS, was distributed diffusely throughout the cells and did not concentrate in nuclei, which is consistent with a requirement for this domain for accumulating Nrg-1-ICD in nuclei. The presence or absence of the second putative NLS (PRLREKK) had no effect on the cellular localization of GFP fusion proteins (unpublished data).

To test further that erbB2:erbB4-induced nuclear targeting of Nrg-1a-ICD was associated with proteolysis of the full-length transmembrane form of Nrg-1, we separated cytoplasmic and membrane fractions from nuclear extracts of HEK293T cells expressing a CRD-Nrg-1βa-HA fusion protein (full-length CRD-Nrg-1βa tagged at the COOH terminus with an 11–amino acid HA epitope). The Nrg-1 COOH terminus was detected by probing immunoblots with an anti-HA antibody. In cells incubated under control conditions (untreated or treated with soluble erbB2; Fig. 4 C, erbB2), the ~110-kD full-length protein and several higher molecular mass bands were detected. These higher molecular mass bands likely correspond to highly glycosylated or possibly aggregated forms of Nrg-1(Wang et al., 2001). Treatment of transfected cells with soluble erbB2 + erbB4 resulted in increased amounts of a mostly nuclear ~50-kD protein corresponding to the Nrg-1-ICD (Fig. 4 C, erbB2:B4).

As a further demonstration that the Nrg-1-ICD translocates into nuclei, we expressed fusion proteins comprised of CRD-Nrg-1βa and the chimeric transcription factor Gal4-VP16 (Nrg-1βa-Gal4-VP16), Nrg-1βa-ICD (lacking the ECD and the transmembrane domains) plus the DNA-binding domain from Gal4 (ICD-Gal4), but without the VP16 activation domain, or Nrg-1βa-$ICD_{\Delta NLS}$ plus the Gal4 DNA-binding domain ($ICD_{\Delta NLS}$-Gal4). The distribution of these fusion proteins in HEK 293T cells was measured by assaying luciferase expression from a cotransfected

Gal4-UAS–luciferase reporter plasmid (Fig. 5). Expression of the nonmembrane-tethered Nrg-1-ICD-$Gal4_{DBD}$ chimera increased luciferase activity ~10-fold compared with the full-length Nrg-1 fused to Gal4-VP16 or compared with Nrg-1-$ICD_{\Delta NLS}$-$Gal4_{DBD}$ (Fig. 5 B; 33-fold vs. fourfold or 2.8-fold, respectively). This level of transactivation is roughly comparable to the levels seen in cells expressing a $Gal4_{DBD}$-$VP16_{AD}$ chimera. As the $Gal4_{DBD}$ lacks a transactivation domain and a nuclear localization signal, luciferase activity indicates that the Nrg-1-ICD has an interaction domain that is able to recruit coactivators to the Gal4-UAS promoter.

The appearance of a ~50-kD COOH-terminal fragment of Nrg-1 in nuclei after soluble erbB2:erbB4 (Fig. 2 C and Fig. 4 C) or after depolarization (Fig. 2 C) is consistent with regulated cleavage of the transmembrane precursor form of CRD-Nrg-1. Constitutive and regulated extracellular cleavage of both type 1 and type III Nrg-1 has been characterized (Burgess et al., 1995; Lu et al., 1995; Liu et al., 1998b; Loeb et al., 1998; Han and Fischbach, 1999; Montero et al., 2000; Wang et al., 2001), but events leading to the release of the Nrg-1-ICD from the membrane have not been studied. Because the first eight intracellular amino acids are required for nuclear translocation, the cleavage event that releases the ICD is expected to occur at the junction between this sequence and the transmembrane domain, or within the transmembrane domain. As such, we tested whether γ-secretases, enzymes known to catalyze intramembranous proteolysis (Struhl and Adachi, 1998, 2000; Struhl and Greenwald, 1999, 2001; Brown et al., 2000; Ni et al., 2001; Ebinu and Yankner, 2002; Lee et al., 2002), might be involved in Nrg-1-ICD processing. HEK 293T cells expressing CRD-Nrg-1βa-Gal4-VP16 were pretreated with γ-secretase inhibitors (Fig. 5; inhibitors 1, CM-265; 2, WPE(III)-36B; or 3, MW (III)-26A) for 8 h before treatment with soluble erbB2 + erbB4. In the absence of inhibitors, or in cells treated with an inactive analogue of these inhibitors (JT-326), exposure of cells to soluble erbB2:erbB4 significantly elevated luciferase levels (Fig. 5 C, columns 3 and 9 compared with columns 1, 2, or 5). The induction of luciferase expression was blocked by all three inhibitors, as well as by preincubating soluble erbB2:erbB4 with the CRD-Nrg-1 ECD. Therefore, the stimulated nuclear targeting of the CRD-Nrg-1-ICD, at least in part, is dependent on a γ-secretase–like activity. These results are consistent with a model in which CRD-Nrg-1–erbB interactions result in cleavage of Nrg-1 within the transmembrane domain and the subsequent release and nuclear targeting of the Nrg-1-ICD.

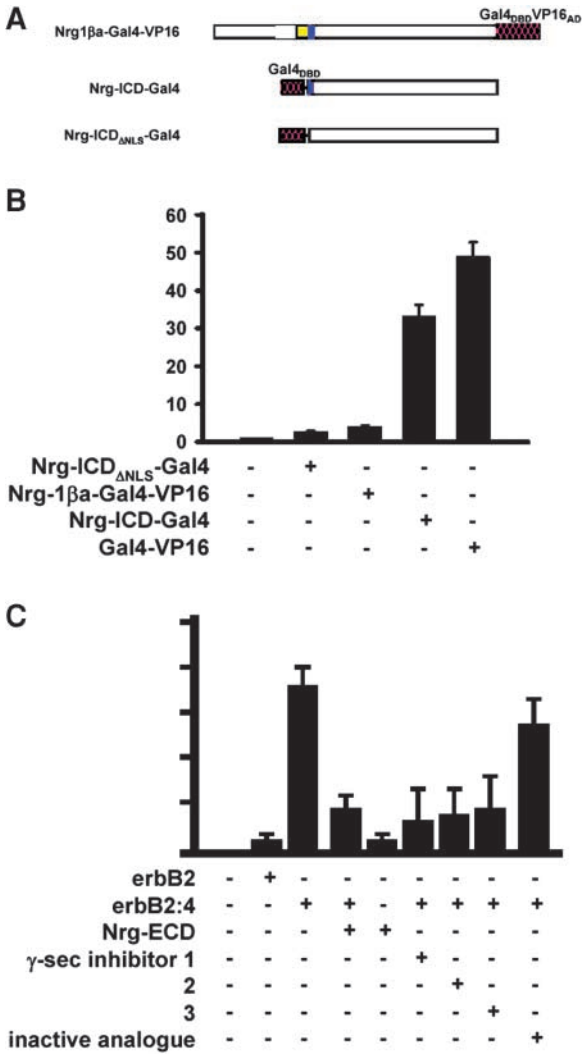

Figure 5. **Treatment of transfected cells with soluble erbB receptors stimulates Nrg-1-ICD cleavage and translocation to a transcriptionally active compartment.** (A) Schematic illustrations showing organization of the Gal4-Nrg-1 fusion proteins used. Gal4, DNA-binding domain; VP16, activation domain from the Herpes virus VP16 transcription factor. (B) Nrg-1βa-Gal4-VP16, Nrg-ICD-$Gal4_{DBD}$, Nrg-$ICD_{\Delta NLS}$-$Gal4_{DBD}$, Nrg-1-ICD, or $Gal4_{DBD}$-$VP16_{AD}$ expression plasmids or empty vector (control) were cotransfected into HEK293T cells with a reporter plasmid containing four copies of the Gal4 UAS fused to the luciferase coding region. Luciferase activities were measured 48 h after transfection and values normalized to the control levels (±SEM). Membrane tethering (Nrg-1-Gal4-VP16) or exclusion from the nucleus (Nrg-1-$ICD_{\Delta NLS}$-$Gal4_{DBD}$) reduced the Nrg-1-ICD-Gal4 transcriptional activity by over 10-fold. (C) The NRG-1βa-Gal4-VP16–expressing plasmid was cotransfected into HEK293T cells with the Gal4-UAS–luciferase reporter. Cells were treated with one of three γ-secretase inhibitors or an inactive analogue of these inhibitors from 24–48 h after transfection. For the final 8 h before measuring, luciferase activity cells also were treated with soluble erbB2, soluble erbB2 + erbB4 (erbB2:B4), erbB2:B4 preincubated with the ECD of CRD-Nrg-1 (NRG-ECD), or CRD-Nrg-1 ECD alone. Luciferase levels (±SEM) were normalized to control (untreated cells cotransfected with reporter and Nrg-1-Gal4-VP16 plasmids = 1).

Discussion

The principle finding of our studies is that CRD-Nrg-1 is a bidirectional signaling molecule. Interaction of the Nrg-1 ECD with erbB receptors results in well-characterized signaling in the erbB-expressing target cells. In neurons, Nrg-1 processing and Nrg-1-ICD nuclear targeting are regulated by either interaction with erbB2–erbB4 or by depolarization, and results in altered gene expression. Stimulated nuclear translocation of Nrg-1-ICD depends on an activity that is sensitive to γ-secretase inhibitors. It is striking that in our original cDNA screen we found that four of the six target genes encode products involved in either apoptosis or in cell cycle progression, and that nuclear targeting of the Nrg-1-ICD prevents neuronal apoptosis. Together, these results

support the proposal that erbB–Nrg-1 interactions elicit a Nrg-1-ICD signaling cascade important to neuronal survival. This proposed signaling mechanism could explain the loss of Nrg-1–expressing neurons that have been consistently reported in mice in which all, or part, of the Nrg-1 gene has been disrupted (Kramer et al., 1996; Erickson et al., 1997; Meyer et al., 1997; Britsch et al., 1998; Wolpowitz et al., 2000).

Our current working model of CRD-Nrg-1 signaling is schematized in Fig. 6. Transmembrane Nrg-1 and erbB receptors are expressed on the surface of neighboring cells. After binding to the Nrg-1 EGF-like domain, erbB4 (predominantly on target neurons or erbB3 on glia—not depicted for simplicity) dimerizes, most likely with erbB2 (Fig. 6, steps 1 and 2). As a result, the erbB receptors are activated and forward signaling occurs (Fig. 6, step 6). In addition, formation of this complex results in cleavage of Nrg-1, possibly in both the external juxtamembrane region releasing the EGF-like domain (Fig. 6, step 3), and in the transmembrane domain (Fig. 6, step 4). The details of the cleavage events are unclear. To date, we have focused our studies on CRD-Nrg-1 and not Ig-Nrg-1. The processing of transmembrane CRD- and Ig-Nrg-1 differs. The CRD domain provides a second membrane interaction domain (Wang et al., 2001; Cabedo et al., 2002). Recent results in transfected cells indicate that CRD-Nrg-1 initially presents in a hairpin-like configuration at the cell surface with both the NH_2 terminus and COOH terminus in the cytoplasm, with part of the CRD domain forming an NH_2-terminal transmembrane domain. Cleavage in the "stalk" region yields two molecules, each with a single transmembrane domain (Wang et al., 2001). In this scenario, the EGF-like domain that interacts with the erbB receptors and the ICD implicated in back signaling are parts of separate polypeptides. If this topology is dominant in neurons, then these two polypeptides must remain physically associated if EGF-like domain binding to erbB receptors is to elicit proteolysis in the second transmembrane domain. The results of double staining of neurons with antibodies recognizing either the ECD or the ICD, of Nrg-1 (Fig. 2 A) and subcellular fractionation data support this conclusion. Before treatment with soluble erbB2 + erbB4, the Nrg-1 extracellular and ICDs colocalize on neuronal processes. After treatment, both domains cluster and the intracellular clusters occupy new positions distinct from the ECDs.

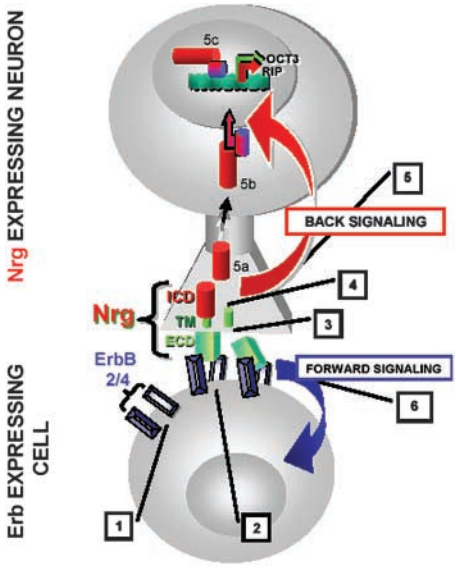

Figure 6. **Bidirectional signaling by transmembrane Nrg-1.** Both forward and back signaling result from interactions between erbB receptors (blue) and membrane-tethered Nrg-1 (green and red). Interaction (steps 1 and 2) results in activation of erbB receptor tyrosine kinases and subsequent induction of target genes (step 6) in erbB-expressing cells, as well as intramembranous (and possibly extracellular) cleavage of Nrg-1 (steps 3 and 4). The released Nrg-1-ICD (red) translocates from neurites to cell bodies (step 5a), and then to the nucleus, possibly with other proteins (step 5b), where it regulates target gene expression (step 5c). See the Discussion for further details of this model.

Although Ig-Nrg-1 can signal as transmembrane proteins (Aguilar and Slamon, 2001), the Ig-EGF–like ECD is readily released from the transmembrane precursor, both under basal conditions and in response to activation of PKC and MAPK (Loeb et al., 1998; Han and Fischbach, 1999; Wang et al., 2001). At present, we do not know whether Ig-Nrg-1 is involved in back signaling, and if so, whether the same biological response is elicited. It is noteworthy that ectopic expression of transmembrane Ig-Nrg-1 in nonneuronal cells, in vitro and in vivo, increases apoptosis and that the apoptotic response is ICD-dependent (Grimm and Leder, 1997; Grimm et al., 1998; Weinstein et al., 1998; Weinstein and Leder, 2000). Whether the pro- versus antiapoptotic signals represent differences in cell types studied or differences in Ig- versus CRD-Nrg-1 back signaling is not known.

After cleavage and release from the plasma membrane, the Nrg-1-ICD translocates to the nucleus (Fig. 6, step 5). This nuclear translocation is associated with changes in gene expression and cellular phenotype. As a component of a $Gal4_{DBD}$-Nrg-1-ICD fusion protein, the Nrg-1-ICD has transcriptional transactivation activity (Fig. 5). Whether this is a true property of the Nrg-1-ICD or simply a consequence of the presence of protein interaction domains within the Nrg-1-ICD that allows the fusion protein to interact with bona fide transactivators, is not known. Examination of the Nrg-1-ICD sequence failed to identify any obvious DNA-binding or transcriptional activation motifs, and the question of whether this protein has inherent transcriptional regulatory properties needs to be addressed experimentally. Within the context of our working model, we propose that Nrg-1-ICD physically interacts with an unidentified transcription factor, either before entering the nucleus (Fig. 6, step 5 b) or in the nucleus (Fig. 6, step 5 c).

Although the model depicted in Fig. 6 implies that all back signaling that is transduced by the Nrg-1-ICD involves nuclear translocation, we cannot rule out other nonnuclear targets for the released Nrg-1-ICD. Two possible binding partners for the Nrg-1-ICD that have been described include LIM kinase 1 (LIMK1; Wang et al., 1998) and a second zinc finger–containing protein related to PLZF (CNIP; unpublished data). The Nrg-1-ICD–LIMK1 interaction is believed to occur at synapses where LIMK1 is involved in regulating actin reorganization and neurite outgrowth (Arber et al., 1998; Wang et al., 1998, 2000; Yang et al., 1998a; Aizawa et al., 2001). LIMK1 also shuttles between the nu-

cleus and cytoplasm (Yang and Mizuno, 1999), and is linked, via the actin cytoskeleton, to transcriptional regulation (Geneste et al., 2002). Whether Nrg-1-ICD interactions affect LIMK1 function, or whether LIMK1 is a significant component of the Nrg-1-ICD back-signaling pathway, is not known.

A number of recent papers have added to the growing list of transmembrane proteins that have ICDs released by regulated intramembranous proteolysis (Brown and Goldstein, 1997; Brown et al., 2000; Jeffries and Capobianco, 2000; Ebinu and Yankner, 2002; Lee et al., 2002; Leissring et al., 2002). Based on our results, CRD-Nrg-1 should be added to this list. In the nervous system, CRD-Nrg-1 (or Ig-Nrg-1) and erbB4 (and possibly erbB3) constitute a bidirectional signaling module, reminiscent of other proteins involved in neuronal development and function, notably ephrin B ligands and Eph receptors (Lu et al., 2001; Schmucker and Zipursky, 2001). What is apparently unique to the CRD-Nrg-1–erbB4 system is the coupling of classical receptor tyrosine kinase signaling in one direction with the regulated release of a transcriptional regulator from a membrane-tethered precursor in the other direction.

Materials and methods

Neuronal cultures

All culture media and supplements were purchased from GIBCO BRL. Spiral ganglia from E13–E16 mouse embryos were dissociated mechanically into a single cell suspension after digestion with trypsin. The cells were recovered by centrifugation (1,000 *g* for 8 min) and the pellet resuspended in culture medium consisting of Neurobasal-A medium supplemented with B-27 and 0.5 mM L-glutamine. The suspension was seeded on a 6-ml dish or laminin-coated (0.01 mg/ml) plastic coverslips at 400,000 cells/ml. For the hippocampal neuronal culture, the hippocampus was dissected from E16 mouse brain and dispersed after trypsin digestion. Cells were plated (150,000 cells/6-cm plastic petri dish) in neurobasal medium. Cultures were maintained at 37°C in an atmosphere containing 5% CO_2.

Soluble erbB receptors were prepared by transfecting HEK293 cells with plasmids encoding chimeras between human erbB2 (residues 20–645) or erbB4 (26–640) and the Fc domain of human IgG (Genentech, Inc.). After 48 h, conditioned media were collected and either concentrated and used as such, or fusion proteins were purified using protein A–agarose. Purity and concentrations were assessed by immunoblotting and silver staining after separation of 7.5% SDS–polyacrylamide gels. Soluble erbB2 and erbB4 were used at ~10 μg/ml final concentrations.

Analysis of gene expression

Total RNA isolated from untreated and soluble erbB2 + erbB4–treated E13.5 cultures of sensory neurons of spiral ganglia, was labeled with ^{32}P using the Atlas Pure Total RNA Labeling System (CLONTECH Laboratories, Inc.) and hybridized to Atlas Mouse 1.2 arrays (CLONTECH Laboratories, Inc.). After a high stringency wash and autoradiography, differences between the two hybridization patterns were noted. Total RNA from E13.5 SGN cultures was used for RT-PCR. PCR reactions were performed for 35 cycles (45 s at 94°C, 60 s at 52°C, and 90 s at 72°C) in a volume of 25 μl containing 1× PCR buffer, 100 μM dNTPs, 1 μM each primer, and 1 U Taq polymerase (Boehringer). Reactions were done in triplicate. Amplified products were separated on 3% NuSeive agarose gels and the band intensity was compared with amplified actin bands. Samples processed in parallel, but without reverse transcriptase added were used as negative controls. In initial experiments, amplified bands were purified and sequenced to confirm their identity.

Immunostaining

Neuronal cultures were fixed with 4% PFA and 4% sucrose in PBS for 15 min, and permeabilized with 0.25% Triton X-100 in PBS for 5 min. The cells were washed three times in PBS and incubated in 10% normal goat serum for 1 h at 37°C. Cells were incubated overnight at 4°C in primary antibodies in PBS with 3% normal goat serum (Nrg-ICD, 1:1,000, sc-348 or sc-537 [Santa Cruz Biotechnology, Inc.]; Nrg ECD, MS-272-P [Neomarkers]; neurofilaments, 1:2,000, NCL-NF68 and NCL-NF160 [Novocastra Lab.]; MAP-2, sc-5357 [Santa Cruz Biotechnology, Inc.]). The cells were washed and incubated with rhodamine- or FITC-conjugated secondary antibodies (1:1,000; Jackson ImmunoResearch Laboratories) and TOTO-3 (1 μM, Molecular Probes) for 1 h at 37°C. The cells were viewed with a confocal argon/krypton laser microscope (model LSM 410; Carl Zeiss MicroImaging, Inc.). Data were collected from stacks of ≤1-μM sections.

Cellular fractionation

Cytoplasmic, particulate, and nuclear fractions were prepared using "Nuclear and Cytoplasmic extraction reagents" (Pierce Chemical Co.). Protein concentrations of each sample were measured by the Bradford method. 40 μg of nuclear, 40 μg of particulate, and 120 μg of cytoplasmic proteins were separated on 10% SDS-PAGE, transferred to nitrocellulose membranes (Schleicher & Schuell), and probed with antibodies against Nrg-1-ICD, histone H1, or eIF5. Apparent molecular mass was estimated by comparing the relative mobility of immunoreactive bands to prestained SDS-PAGE standards (Low Range; Bio-Rad Laboratories).

Plasmid constructs

Epitope-tagged full-length or truncated forms of NRG-β1a were prepared by the PCR and cloned into pcDNA3.1/V5/His-TOPO or pcDNA3.1/CT-GFP-TOPO (Invitrogen). The primer pair for fusing full-length CRD-NRG-β1a to the HA epitope was 5′-ACCATGTCTGAGGGAGCTGGCGGGAGGT-3′ and 3′-TCATACAGCGTAGTCTGGGACGTCGTATGGGTA-5′. The PCR primer pair used to fuse full-length NRG-1βa to GFP was 5′-AGCATGGCTGAGAAGAAGAAGGAAAAA-3′ and 3′-TACAGCAATGGGGTCTTGATTCGTTATTACACT-5′. The PCR primer pair used to fuse the cytoplasmic domain containing the putative NLS-1 (aa 295–390) to GFP was 5′-ATTATGAAAACCAAGAAACAGAGA-3′ and 3′-GACCATTACTCCAGCTGTGACTTG-5′. The PCR primer pair used to fuse the cytoplasmic domain lacking NLS-1 (aa 304–390) to GFP was 5′-ATTATGTTGAATGACCGTTTAAGA-3′ and 3′-GACCATTACTCCAGCTGTGACTTG-5′. GAL4-VP16 was fused in frame to the COOH terminus of full-length NRG-1βa and was cloned by the PCR into pcDNA3.1/V5/His-TOPO (Invitrogen). Primer pairs used for amplification of Gal4-VP16 were 5′-GTATACCCATACCCGCCGAAGCTT-3′ and 3′-CTTATACTCCACCGTACTCGTCAA-5′; and for amplification of NRG-β1a were 5′-ATGGCTGAGAAGAAGAAGGAAAAAGAA-3′ and 3′-GTATGGGTATACAGCAATGGGGTCTTG-5′. DNA sequences were confirmed. Note that in each construct, the COOH terminus was engineered to retain the IAV sequence of the Nrg-1-ICD-a form because similar sequences have been implicated in targeting and processing of other transmembrane growth factors.

Luciferase assay

A 10-μg plasmid containing four copies of the Gal4-UAS element fused to the firefly luciferase coding region (p4Luc from R. Evans, Salk Institute, La Jolla, CA) was cotransfected into 293T cells with 20 μg NRG-β1a-Gal4-VP16 or 20 μg NRG-1-ICD-$Gal4_{DBD}$ and 2 μg pcDNA-GFP (used to determine transfection efficiency). Luciferase activity was measured in lysates 48 h after transfection. Where indicated, γ-secretase inhibitors (from D. Selkoe and M. Wolfe, Harvard Medical School, Boston, MA) were added for the final 24 h.

We thank Jean Gautier and Gary Struhl for insightful discussions. J. Bao thanks Robin Davis for instruction in culturing SGNs, and thanks D. Selkoe and M. Wolfe for providing γ-secretase inhibitors.

This work was supported by the National Institutes of Health grants NS29071, CA79737, DK07715, and AG01016.

Submitted: 17 December 2002
Revised: 24 April 2003
Accepted: 24 April 2003

References

Aguilar, Z., and D.J. Slamon. 2001. The transmembrane heregulin precursor is functionally active. *J. Biol. Chem.* 276:44099–44107.

Aizawa, H., S. Wakatsuki, A. Ishii, K. Moriyama, Y. Sasaki, K. Ohashi, Y. Sekine-Aizawa, A. Sehara-Fujisawa, K. Mizuno, Y. Goshima, and I. Yahara. 2001. Phosphorylation of cofilin by LIM-kinase is necessary for semaphorin 3A-induced growth cone collapse. *Nat. Neurosci.* 4:367–373.

Arber, S., F.A. Barbayannis, H. Hanser, C. Schneider, C.A. Stanyon, O. Bernard,

and P. Caroni. 1998. Regulation of actin dynamics through phosphorylation of cofilin by LIM-kinase. *Nature.* 393:805–809.

Britsch, S., L. Li, S. Kirchhoff, F. Theuring, V. Brinkmann, C. Birchmeier, and D. Riethmacher. 1998. The ErbB2 and ErbB3 receptors and their ligand, neuregulin-1, are essential for development of the sympathetic nervous system. *Genes Dev.* 12:1825–1836.

Brown, M.S., and J.L. Goldstein. 1997. The SREBP pathway: regulation of cholesterol metabolism by proteolysis of a membrane-bound transcription factor. *Cell.* 89:331–340.

Brown, M.S., J. Ye, R.B. Rawson, and J.L. Goldstein. 2000. Regulated intramembrane proteolysis: a control mechanism conserved from bacteria to humans. *Cell.* 100:391–398.

Buonanno, A., and G.D. Fischbach. 2001. Neuregulin and ErbB receptor signaling pathways in the nervous system. *Curr. Opin. Neurobiol.* 11:287–296.

Burgess, T.L., S.L. Ross, Y.X. Qian, D. Brankow, and S. Hu. 1995. Biosynthetic processing of neu differentiation factor. Glycosylation trafficking, and regulated cleavage from the cell surface. *J. Biol. Chem.* 270:19188–19196.

Cabedo, H., C. Luna, A.M. Fernandez, J. Gallar, and A. Ferrer-Montiel. 2002. Molecular determinants of the sensory and motor neuron-derived factor insertion into plasma membrane. *J. Biol. Chem.* 277:19905–19912.

Cao, X., and T.C. Sudhof. 2001. A transcriptionally (correction of transcriptively) active complex of APP with Fe65 and histone acetyltransferase Tip60. *Science.* 293:115–120.

Carraway, K.L., III. 1996. Involvement of the neuregulins and their receptors in cardiac and neural development. *Bioessays.* 18:263–266.

Ebinu, J.O., and B.A. Yankner. 2002. A RIP tide in neuronal signal transduction. *Neuron.* 34:499–502.

Erickson, S.L., K.S. O'Shea, N. Ghaboosi, L. Loverro, G. Frantz, M. Bauer, L.H. Lu, and M.W. Moore. 1997. ErbB3 is required for normal cerebellar and cardiac development: a comparison with ErbB2- and heregulin-deficient mice. *Development.* 124:4999–5011.

Fitzpatrick, V.D., P.I. Pisacane, R.L. Vandlen, and M.X. Sliwkowski. 1998. Formation of a high affinity heregulin binding site using the soluble extracellular domains of ErbB2 with ErbB3 or ErbB4. *FEBS Lett.* 431:102–106.

Geneste, O., J.W. Copeland, and R. Treisman. 2002. LIM kinase and Diaphanous cooperate to regulate serum response factor and actin dynamics. *J. Cell Biol.* 157:831–838.

Grimm, S., and P. Leder. 1997. An apoptosis-inducing isoform of neu differentiation factor (NDF) identified using a novel screen for dominant, apoptosis-inducing genes. *J. Exp. Med.* 185:1137–1142.

Grimm, S., E.J. Weinstein, I.M. Krane, and P. Leder. 1998. Neu differentiation factor (NDF), a dominant oncogene, causes apoptosis in vitro and in vivo. *J. Exp. Med.* 188:1535–1539.

Han, B., and G.D. Fischbach. 1999. Processing of ARIA and release from isolated nerve terminals. *Philos. Trans. R. Soc. Lond. B Biol. Sci.* 354:411–416.

Jeffries, S., and A.J. Capobianco. 2000. Neoplastic transformation by Notch requires nuclear localization. *Mol. Cell. Biol.* 20:3928–3941.

Kimberly, W.T., J.B. Zheng, S.Y. Guenette, and D.J. Selkoe. 2001. The intracellular domain of the beta-amyloid precursor protein is stabilized by Fe65 and translocates to the nucleus in a notch-like manner. *J. Biol. Chem.* 276: 40288–40292.

Kramer, R., N. Bucay, D.J. Kane, L.E. Martin, J.E. Tarpley, and L.E. Theill. 1996. Neuregulins with an Ig-like domain are essential for mouse myocardial and neuronal development. *Proc. Natl. Acad. Sci. USA.* 93:4833–4838.

Lee, H.J., K.M. Jung, Y.Z. Huang, L.B. Bennett, J.S. Lee, L. Mei, and T.W. Kim. 2002. Presenilin-dependent γ-secretase-like intramembrane cleavage of ErbB4. *J. Biol. Chem.* 277:6318–6323.

Lee, K.F., H. Simon, H. Chen, B. Bates, M.C. Hung, and C. Hauser. 1995. Requirement for neuregulin receptor erbB2 in neural and cardiac development. *Nature.* 378:394–398.

Leimeroth, R., C. Lobsiger, A. Lussi, V. Taylor, U. Suter, and L. Sommer. 2002. Membrane-bound neuregulin 1 type III actively promotes Schwann cell differentiation of multipotent Progenitor cells. *Dev. Biol.* 246:245–258.

Leissring, M.A., M.P. Murphy, T.R. Mead, Y. Akbari, M.C. Sugarman, M. Jannatipour, B. Anliker, U. Muller, P. Saftig, B. De Strooper, et al. 2002. A physiologic signaling role for the gamma-secretase-derived intracellular fragment of APP. *Proc. Natl. Acad. Sci. USA.* 99:4697–4702.

Liu, X., H. Hwang, L. Cao, M. Buckland, A. Cunningham, J. Chen, K.R. Chien, R.M. Graham, and M. Zhou. 1998a. Domain-specific gene disruption reveals critical regulation of neuregulin signaling by its cytoplasmic tail. *Proc. Natl. Acad. Sci. USA.* 95:13024–13029.

Liu, X., H. Hwang, L. Cao, D. Wen, N. Liu, R.M. Graham, and M. Zhou. 1998b. Release of the neuregulin functional polypeptide requires its cytoplasmic tail. *J. Biol. Chem.* 273:34335–34340.

Loeb, J.A., E.T. Susanto, and G.D. Fischbach. 1998. The neuregulin precursor proARIA is processed to ARIA after expression on the cell surface by a protein kinase C-enhanced mechanism. *Mol. Cell. Neurosci.* 11:77–91.

Lu, H.S., S. Hara, L.W. Wong, M.D. Jones, V. Katta, G. Trail, A. Zou, D. Brankow, S. Cole, S. Hu, et al. 1995. Post-translational processing of membrane-associated neu differentiation factor proisoforms expressed in mammalian cells. *J. Biol. Chem.* 270:4775–4783.

Lu, Q., E.E. Sun, R.S. Klein, and J.G. Flanagan. 2001. Ephrin-B reverse signaling is mediated by a novel PDZ-RGS protein and selectively inhibits G protein-coupled chemoattraction. *Cell.* 105:69–79.

Meyer, D., and C. Birchmeier. 1995. Multiple essential functions of neuregulin in development. *Nature.* 378:386–390.

Meyer, D., T. Yamaai, A. Garratt, E. Riethmacher-Sonnenberg, D. Kane, L.E. Theill, and C. Birchmeier. 1997. Isoform-specific expression and function of neuregulin. *Development.* 124:3575–3586.

Montero, J.C., L. Yuste, E. Diaz-Rodriguez, A. Esparis-Ogando, and A. Pandiella. 2000. Differential shedding of transmembrane neuregulin isoforms by the tumor necrosis factor-alpha-converting enzyme. *Mol. Cell. Neurosci.* 16: 631–648.

Murphy, S., R. Krainock, and M. Tham. 2002. Neuregulin signaling via erbB receptor assemblies in the nervous system. *Mol. Neurobiol.* 25:67–77.

Ni, C.Y., M.P. Murphy, T.E. Golde, and G. Carpenter. 2001. gamma-Secretase cleavage and nuclear localization of ErbB-4 receptor tyrosine kinase. *Science.* 294:2179–2181.

Pinkas-Kramarski, R., M. Shelly, B.C. Guarino, L.M. Wang, L. Lyass, I. Alroy, M. Alimandi, A. Kuo, J.D. Moyer, S. Lavi, et al. 1998. ErbB tyrosine kinases and the two neuregulin families constitute a ligand-receptor network. *Mol. Cell. Biol.* 18:6090–6101.

Schmucker, D., and S.L. Zipursky. 2001. Signaling downstream of Eph receptors and ephrin ligands. *Cell.* 105:701–704.

Struhl, G., and A. Adachi. 1998. Nuclear access and action of notch in vivo. *Cell.* 93:649–660.

Struhl, G., and A. Adachi. 2000. Requirements for presenilin-dependent cleavage of notch and other transmembrane proteins. *Mol. Cell.* 6:625–636.

Struhl, G., and I. Greenwald. 1999. Presenilin is required for activity and nuclear access of Notch in *Drosophila*. *Nature.* 398:522–525.

Struhl, G., and I. Greenwald. 2001. Presenilin-mediated transmembrane cleavage is required for Notch signal transduction in *Drosophila*. *Proc. Natl. Acad. Sci. USA.* 98:229–234.

Wang, J.Y., K.E. Frenzel, D. Wen, and D.L. Falls. 1998. Transmembrane neuregulins interact with LIM kinase 1, a cytoplasmic protein kinase implicated in development of visuospatial cognition. *J. Biol. Chem.* 273:20525–20534.

Wang, J.Y., D.J. Wigston, H.D. Rees, A.I. Levey, and D.L. Falls. 2000. LIM kinase 1 accumulates in presynaptic terminals during synapse maturation. *J. Comp. Neurol.* 416:319–334.

Wang, J.Y., S.J. Miller, and D.L. Falls. 2001. The N-terminal region of neuregulin isoforms determines the accumulation of cell surface and released neuregulin ectodomain. *J. Biol. Chem.* 276:2841–2851.

Weinstein, E.J., and P. Leder. 2000. The extracellular region of heregulin is sufficient to promote mammary gland proliferation and tumorigenesis but not apoptosis. *Cancer Res.* 60:3856–3861.

Weinstein, E.J., S. Grimm, and P. Leder. 1998. The oncogene heregulin induces apoptosis in breast epithelial cells and tumors. *Oncogene.* 17:2107–2113.

Wolpowitz, D., T.B. Mason, P. Dietrich, M. Mendelsohn, D.A. Talmage, and L.W. Role. 2000. Cysteine-rich domain isoforms of the neuregulin-1 gene are required for maintenance of peripheral synapses. *Neuron.* 25:79–91.

Yang, N., and K. Mizuno. 1999. Nuclear export of LIM-kinase 1, mediated by two leucine-rich nuclear-export signals within the PDZ domain. *Biochem. J.* 338: 793–798.

Yang, N., O. Higuchi, K. Ohashi, K. Nagata, A. Wada, K. Kangawa, E. Nishida, and K. Mizuno. 1998a. Cofilin phosphorylation by LIM-kinase 1 and its role in Rac-mediated actin reorganization. *Nature.* 393:809–812.

Yang, X., Y. Kuo, P. Devay, C. Yu, and L. Role. 1998b. A cysteine-rich isoform of neuregulin controls the level of expression of neuronal nicotinic receptor channels during synaptogenesis. *Neuron.* 20:255–70.